The Effect of AC Zeeman Frequency Shifts Due to the NMR RF Field Used for AFP in EPR-Frequency-Shift ^{3}He Polarimetry

Jaideep Singh, Peter Dolph, & Al Tobias
University of Virginia
Version 0.70

March 24, 2009

Abstract

We can determine the ^{3}He polarization inside polarized ^{3}He target cells by measuring the frequency shift in the EPR spectrum of alkali atoms. This shift is mostly due to the effective magnetic field associated with spin-exchange collisions with the polarized ^{3}He nuclei. Since we can only directly measure the EPR frequency due to the total magnetic field felt by the alkali atoms, we change the sign of the frequency shift by flipping the ^{3}He spins using the NMR technique of frequency sweep adiabatic fast passage (AFP). If all else is equal, then the difference in EPR frequencies for the two directions of the ^{3}He spins isolates the frequency shift due to the polarized ^{3}He nuclei: $\nu^{\uparrow}_{\mathtt{EPR}} - \nu^{\downarrow}_{\mathtt{EPR}} = \Delta\nu_{\mathtt{EPR}} = 2 \times (\Delta\nu)_{\mathrm{He}}$.

What complicates this analysis is the fact that the oscillating NMR RF field used for AFP also causes a small frequency shift $(\Delta\nu)_{\mathtt{rf}}$, in this case, due to the AC Zeeman effect. If the magnitude of the NMR RF field changes during AFP, then its corresponding frequency shift is different for the two directions of the ^{3}He spins. Under this condition, the partially canceled frequency shift due to the NMR RF field also contributes to & contaminates the EPR frequency difference: $\Delta\nu_{\mathtt{EPR}} = 2 \times (\Delta\nu)_{\mathrm{He}} + [(\Delta\nu)^{\uparrow}_{\mathtt{rf}} - (\Delta\nu)^{\downarrow}_{\mathtt{rf}})]$. This could potentially be a large systematic error in the determination of the ^{3}He polarization. We'll (1) describe the problem in more detail, (2) calculate the absolute size of the frequency shifts due to the polarized ^{3}He nuclei & the NMR RF fields used for AFP and (3) present an the experimental study of this effect. Finally, we'll note that this effect can be completely eliminated by the measuring the EPR frequencies only when the NMR RF field is turned off.

Contents

1 Description of the "NMR RF Shift" Effect

The result of a typical EPR measurement at UVa is shown in Fig. (1). At the start of an EPR polarization measurement, the total static magnetic field seen by the alkali atoms is $B = B_0 + B_{\mathrm{He}}$, which corresponds to an EPR frequency of:

$$(\nu^{\uparrow}_{\mathtt{EPR}})_{\mathrm{off}} = \nu_0 + (\Delta\nu)_{\mathrm{He}} \tag{1}$$

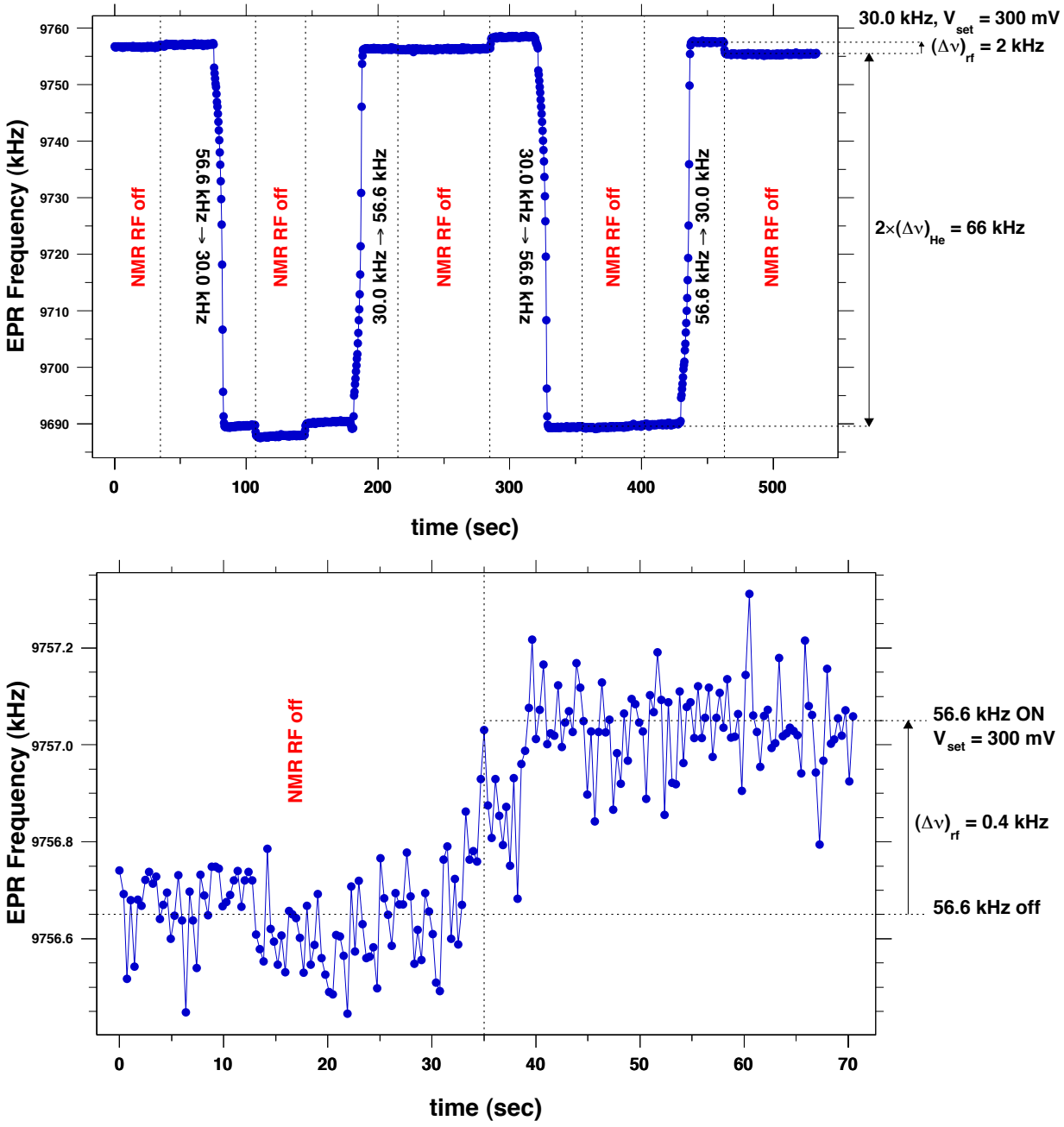

Figure 1: Typical EPR Measurement Sequence. The He spins are flipped using frequency sweep NMR-AFP. The top plot shows the entire data set which includes four ^{3}He spin flips. The shift due to the NMR RF field at 30.0 kHz can be seen at 75 sec $< t <$ 175 sec, 250 sec $< t <$ 325 sec, and finally 425 sec $< t <$ 500 sec. Note that the sign of the RF shift is independent of the direction of the ^{3}He spins. The shift due to the NMR RF field at 56.6 kHz is much smaller, but is visible at 0 sec $< t <$ 70 sec, see the bottom plot. Because the NMR RF coil resonates at about 20 kHz, the amplitude of the RF field at 30.0 kHz is much larger than the amplitude of the RF field at 56.6 kHz for the same function generator set amplitude $V_{\rm set} = 300$ mV.

Under our typical conditions, $B_0 = 13$ G and, for the "well state" transition of ^{39}K, the EPR frequency is around 9.7 MHz. After measuring this EPR frequency for several seconds, the NMR RF field is turned on with a frequency of 56.6 kHz. This NMR RF field causes an additional shift in the EPR frequency:

$$(\nu^{\uparrow}_{\mathtt{EPR}})_{\mathrm{on}} = \nu_0 + (\Delta\nu)_{\mathrm{He}} + (\Delta\nu)^{\uparrow}_{\mathtt{rf}} \tag{2}$$

After again measuring the EPR frequency for several seconds, the NMR RF frequency is swept over a period of 6 seconds from 56.6 kHz, through resonance at 42.2 kHz, to 30.0 kHz. The rate is chosen to be fast enough to minimize the ^{3}He relaxation at resonance, but slow enough for the ^{3}He spins to follow the effective field in the rotating frame adiabatically. After the spins have been flipped, the total static magnetic field felt by the alkali atoms is $B = B_0 - B_{\mathrm{He}}$ which corresponds to an EPR frequency of:

$$(\nu^{\downarrow}_{\mathtt{EPR}})_{\mathrm{on}} = \nu_0 - (\Delta\nu)_{\mathrm{He}} + (\Delta\nu)^{\downarrow}_{\mathtt{rf}} \tag{3}$$

and then we turn the NMR RF off to measure:

$$(\nu^{\downarrow}_{\mathtt{EPR}})_{\mathrm{off}} = \nu_0 - (\Delta\nu)_{\mathrm{He}} \tag{4}$$

To conclude the EPR measurement, we follow the same steps already mentioned, but in reverse order:

1. turn the NMR RF on at 30.0 kHz
2. measure the EPR frequency
3. sweep the NMR RF frequency from 30.0 kHz to 56.6 kHz
4. measure the EPR frequency
5. turn the NMR RF off
6. measure the EPR frequency

In addition to this measurement sequence, Fig. (1) also shows the results of an analogous measurement sequence for which the NMR frequency sweep from 30.0 kHz to 56.6 kHz and then back to 30.0 kHz. Using these measurements, there are two frequency differences that can be used to extract the ^{3}He polarization:

$$\Delta(\nu_{\mathtt{EPR}})_{\mathrm{on}} = (\nu^{\uparrow}_{\mathtt{EPR}})_{\mathrm{on}} - (\nu^{\downarrow}_{\mathtt{EPR}})_{\mathrm{on}} = 2 \times (\Delta\nu)_{\mathrm{He}} + \left[(\Delta\nu)^{\uparrow}_{\mathtt{rf}} - (\Delta\nu)^{\downarrow}_{\mathtt{rf}})\right] \tag{5}$$

$$\Delta(\nu_{\mathtt{EPR}})_{\mathrm{off}} = (\nu^{\uparrow}_{\mathtt{EPR}})_{\mathrm{off}} - (\nu^{\downarrow}_{\mathtt{EPR}})_{\mathrm{off}} = 2 \times (\Delta\nu)_{\mathrm{He}} \tag{6}$$

If there is no shift associated with the NMR RF field ($(\Delta\nu)^{\uparrow}_{\mathtt{rf}} = (\Delta\nu)^{\downarrow}_{\mathtt{rf}} = 0$) or if the size of frequency shift associated with the NMR RF field stays the same after the ^{3}He spins are flipped ($[(\Delta\nu)^{\uparrow}_{\mathtt{rf}} - (\Delta\nu)^{\downarrow}_{\mathtt{rf}})] = 0$), then the two frequency differences are identical. However, at least at UVa, this is not the case.

Based on Figs. (1) & (2), we'll make the following observations of the what we call "NMR RF Shift" Effect:

1. the size of $(\Delta\nu)_{\mathtt{rf}}$ has no measurable dependence on the sign and magnitude of the ^{3}He polarization
2. the size of $(\Delta\nu)_{\mathtt{rf}}$ at 13 Gauss appears to in the kHz range for both ^{85}Rb and ^{39}K
3. the sign of $(\Delta\nu)_{\mathtt{rf}}$ is positive for both the "well" state transition $-(I + 1/2) \leftrightarrow -(I - 1/2)$ and the "hat" state transition $+(I + 1/2) \leftrightarrow +(I - 1/2)$
4. the size of $(\Delta\nu)_{\mathtt{rf}}$ increases with the NMR RF amplitude and decreases with the NMR RF frequency

Originally, we thought that $(\Delta\nu)_{\mathtt{rf}} \neq 0$ was due to a direct coupling between the NMR RF coils and the photodiode used for EPR. We tested this hypothesis by increasing the distance between the EPR photodiode and the NMR RF coils. The fluorescence from the cell needed as an input to the EPR feedback circuit was captured by an optical fiber instead of the photodiode directly. Because we used a very long optical fiber,

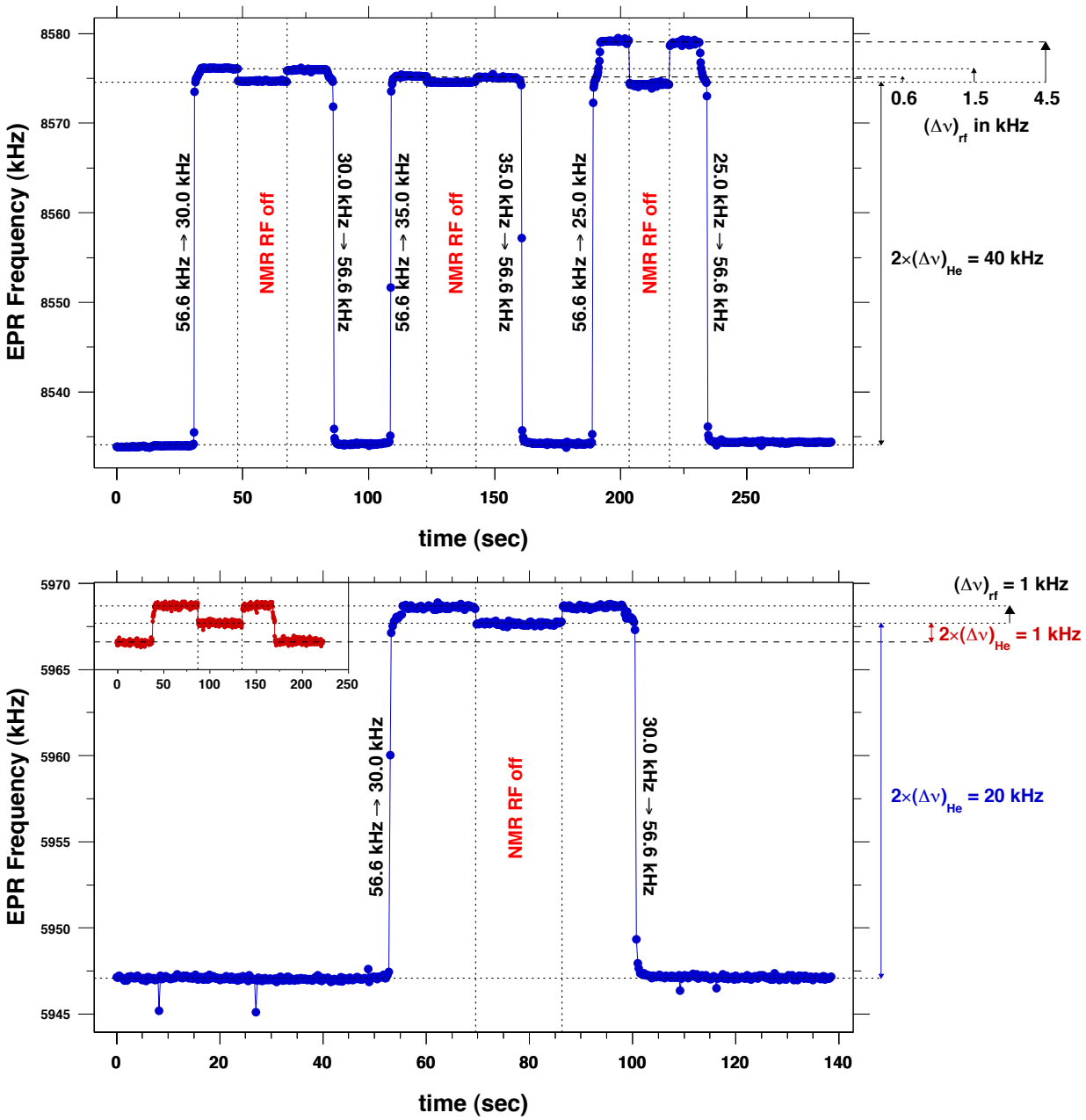

Figure 2: EPR in the High Energy or "Hat" State for ^{39}K (top) and ^{85}Rb (bottom) at 13 Gauss. In the top plot, we see that the shift depends on NMR frequency. This is because circuit used to drive the NMR RF coils resonates at about 20 kHz. In the bottom plot, we see that the NMR RF shift in independent of the size of the shift due to the polarized ^{3}He gas.

the distance between the EPR photodiode and NMR RF coils was several meters. When we performed the EPR measurement under these conditions, we still observed a frequency shift when the NMR RF was turned on and off.

Our new hypothesis (which we believe is correct) is that the NMR RF field directly interacts with the alkali atoms to produce a frequency shift via the AC Zeeman effect. Under our experimental conditions, $B_0 > 10$ Gauss, $\nu_0 > 5$ MHz, $\nu_{\mathtt{rf}} = (40 \pm 20)$ kHz, $B_{\mathtt{rf}} < 0.5$ Gauss, and, using the results of Sec. (3), the size of the shift is given by:

$$(\Delta\nu)_{\mathtt{rf}} = \frac{F(F+1) - m(m-1)}{4\nu_{\mathtt{EPR}}} \left[\frac{\partial\nu}{\partial B} B_{\mathtt{rf}}\right]^2 \tag{7}$$

where $F = I \pm 1/2$, I is the nuclear spin of the alkali atom, $\nu_{\mathtt{EPR}}$ is the frequency of the $|F, m\rangle \leftrightarrow |F, m-1\rangle$ transition, $\partial\nu/\partial B$ is given by Eqn. (9), and $B_{\mathtt{rf}}$ is the amplitude of the NMR RF Field in the lab frame. Tab. (2) lists the quantitative size of the shift for ^{85}Rb and ^{39}K under our conditions. Because, for incidental historical reasons, the NMR RF coils resonate at 20 kHz (see Fig. (3)), the NMR RF field amplitude is higher at 30.0 kHz than at 56.6 kHz for the same set control voltage, which implies $(\Delta\nu)^{\uparrow}_{\mathtt{rf}} \neq (\Delta\nu)^{\downarrow}_{\mathtt{rf}}$. Therefore, in order to avoid all these difficulties, it is much better to use $\Delta(\nu_{\mathtt{EPR}})_{\mathrm{off}}$ than $\Delta(\nu_{\mathtt{EPR}})_{\mathrm{on}}$ to calculate the ^{3}He polarization. To do this, all you have to do is take data with the NMR RF field off before and after the AFP frequency sweep.

2 Calculating the Shift Due to Polarized ^{3}He

More details about the EPR polarimetry method can be found in [1, 2, 3, 4]. To convert from the frequency shift $(\Delta\nu)_{\mathrm{He}}$ to the effective field associated with the polarized ^{3}He , we make the following approximation:

$$B_{\mathrm{He}} = (\Delta\nu)_{\mathrm{He}} \times \left(\frac{\partial\nu}{\partial B}\right)^{-1} \tag{8}$$

Up to fifth order in field, the derivative is:

$$\frac{\partial\nu_{\pm}}{\partial B} = \frac{(g_I\mu_N - g_S\mu_B)}{h[I]} \sum_{n=0}^{5} b_n \frac{x^n}{[I]^n} \tag{9}$$

$$x = (g_I\mu_N - g_S\mu_B)\frac{B}{h\nu_{\mathtt{hfs}}} \tag{10}$$

$$[I] = 2I + 1 \tag{11}$$

$$b_0 = \frac{1 \pm \frac{g_I\mu_N}{g_S\mu_B}([I] \mp 1)}{1 - \frac{g_I\mu_N}{g_S\mu_B}} = 1 \mp \mathcal{O}(10^{-3}) \tag{12}$$

$$b_1 = 2(1 - 2m) \tag{13}$$

$$b_2 = 6\left(1 - 3m + 3m^2 - \frac{[I]^2}{4}\right) \tag{14}$$

$$b_3 = 20\left(1 - 4m + 6m^2 - 4m^3\right) - 6[I]^2(1 - 2m) \tag{15}$$

$$b_4 = 70\left(1 - 5m + 10m^2 - 10m^3 + 5m^4\right) - 25[I]^2\left(1 - 3m + 3m^2\right) + \frac{15[I]^4}{8} \tag{16}$$

$$b_5 = 252\left(1 - 6m + 15m^2 - 20m^3 + 15m^4 - 6m^5\right) - 105[I]^2\left(1 - 4m + 6m^2 - 4m^3\right) + \frac{45[I]^4}{4}(1 - 2m) \tag{17}$$

where I is the nuclear spin, g_I is the nuclear g-factor, μ_N is the nuclear magneton, h is the Planck constant, $[I] = 2I + 1$, and $\nu_{\mathtt{hfs}}$ is the zero-field hyperfine splitting between $F = I + 1/2$ and $F = I - 1/2$, see Tab. (1). For the special case of end transitions, $F = I + 1/2$ and $m = I + 1/2$ for $I + 1/2 \leftrightarrow I - 1/2$ & $m = -I + 1/2$

Isotope	I	**upper** F	**End Transition**	g_I	$\nu_{\mathtt{hfs}}$ MHz
^{6}Li	1	3/2	$s3/2 \leftrightarrow s1/2$	+0.822 056	228.205 26
^{7}Li	3/2	2	$s2 \leftrightarrow s1$	+2.170 960	803.504 09
^{23}Na	3/2	2	$s2 \leftrightarrow s1$	+1.478 347	1 771.626 13
^{39}K	3/2	2	$s2 \leftrightarrow s1$	+0.260 973	461.719 72
^{40}K	4	9/2	$s9/2 \leftrightarrow s7/2$	−0.324 5	-1 142.92
^{41}K	3/2	2	$s2 \leftrightarrow s1$	+0.143 247	254.013 87
^{85}Rb	5/2	3	$s3 \leftrightarrow s2$	+0.541 208	3 035.732 00
^{87}Rb	3/2	2	$s2 \leftrightarrow s1$	+1.834 133	6 834.682 60
^{133}Cs	7/2	4	$s4 \leftrightarrow s3$	+0.736 857	9 192.631 77

Table 1: Hyperfine Structure Data for Alkali Atoms. $F = I + 1/2$ for the upper manifold and $s = \pm$.

for $-I + 1/2 \leftrightarrow -I - 1/2$ and the coefficients for the expansion of the derivative of the EPR frequency are:

$$b_0 = \frac{1 + \frac{g_I \mu_N}{g_S \mu_B}(2I)}{1 - \frac{g_I \mu_N}{g_S \mu_B}} = 1 - \mathcal{O}(10^{-3}) \tag{18}$$

$$b_1 = \mp 4I \tag{19}$$

$$b_2 = 6I\,(2I-1) \tag{20}$$

$$b_3 = \mp 8I\left(4I^2 - 6I + 1\right) \tag{21}$$

$$b_4 = 10I\,(2I-1)\left(4I^2 - 10I + 1\right) \tag{22}$$

$$b_5 = \mp 12I\left(16I^4 - 80I^3 + 80I^2 - 20I + 1\right) \tag{23}$$

where $\pm$ refers to the edge state $m = \pm\left(I + \frac{1}{2}\right)$ involved in the transition. Once we have B_{He}, we can find the He-3 polarization from the effective field due to the He-3 using:

$$B_{\mathrm{He}} = \frac{2\mu_0}{3}\left(\kappa_0 - 1 + \kappa_{\mathrm{geo}}\right)[\mathrm{He}] g_{\mathrm{He}} \mu_N \frac{P_{\mathrm{He}}}{2} \tag{24}$$

where μ_0 is the magnetic permeability of free space, κ_0 is the empirical shift constant, κ_{geo} is a geometric factor, [He] is the He-3 number density, $g_{\mathrm{He}} = -4.254995446$ is the He-3 g-factor, μ_N is the nuclear magneton, $P_{\mathrm{He}} = 2\langle S_z \rangle$ is the He-3 polarization. The values for κ_0 are given by [4, 5]:

$$\mathrm{Rb} : \kappa_0 = 6.39 + 0.00924 \cdot (T - 200\ ^{\circ}\mathrm{C}) \tag{25}$$

$$\mathrm{K} : \kappa_0 = 5.99 + 0.0086 \cdot (T - 200\ ^{\circ}\mathrm{C}) \tag{26}$$

$$\mathrm{Na} : \kappa_0 = 4.84 + 0.00914 \cdot (T - 200\ ^{\circ}\mathrm{C}) \tag{27}$$

The geometric factor κ_{geo} is the ratio of the classical magnetic field produced by the He-3 for the cell geometry averaged over the alkali sampling volume (ASV) to the classical magnetic field produced by a uniformly polarized spherical He-3 sample with the same density and polarization:

$$\kappa_{\mathrm{geo}} = \frac{\frac{1}{V_{\mathrm{ASV}}}\int_{\mathrm{ASV}} \hat{z} \cdot \vec{B}_c \, dV}{\hat{z} \cdot \vec{B}_{\mathrm{sphere}}} \qquad \vec{B}_{\mathrm{sphere}} = \frac{2\mu_0}{3}[\mathrm{He}] g_{\mathrm{He}} \mu_N \frac{P_{\mathrm{He}}}{2} \hat{z} \tag{28}$$

where $\hat{z}$ is the direction of the holding field. The classical field $\vec{B}_c$ can be calculated using the method of magnetic scalar potentials (See section 5.9 of Blue Jackson [6]):

$$\vec{B}_c = \mu_0\left(\vec{H}_c + \vec{M}_c\right) \qquad \vec{H}_c = -\vec{\nabla}\Phi_M \qquad \vec{M}_c = [\mathrm{He}]\frac{g_{\mathrm{He}}\mu_N}{2}\vec{P}_c(\vec{r}) \tag{29}$$

where $\vec{P}_c(\vec{r})$ is the possibly position dependent He polarization vector. For a uniformly polarized region bounded by a surface S, the magnetic scalar potential is given by:

$$\Phi_M(\vec{r}) = \frac{1}{4\pi}\int_S \frac{\hat{n}' \cdot \vec{M}_c(\vec{r}\,')}{|\vec{r} - \vec{r}\,'|}\, dA' \tag{30}$$

where $\hat{n}'$ is the normal unit vector pointing out of S at a position $\vec{r}\,'$ on the surface S. For a region far from the polarized He-3, the magnetic scalar potential is given by:

$$\Phi_M(\vec{r}) = \frac{V\vec{M}_c \times \vec{r}}{4\pi r^3} \tag{31}$$

where V is the total volume of the region containing the polarized He-3. The value of κ_{geo} for a few different geometries are given here:

1. $\kappa_{\text{geo}} = 1$ for a uniformly polarized sphere
2. $\kappa_{\text{geo}} = 3/2$ for an infinitely long cylinder polarized along its axis
3. $\kappa_{\text{geo}} = 3/4$ for an infinitely long cylinder polarized perpendicular to its axis

In quantitative terms, the effective field felt by the alkali metal due to the polarized He-3 vapor is:

$$\begin{aligned} B_{\text{He}} &= \frac{2\mu_0}{3}\left(\kappa_0 - 1 + \kappa_{\text{geo}}\right)[\text{He}] g_{\text{He}}\mu_N \frac{P_{\text{He}}}{2} && (32)\\ &= (-14.5 \text{ milligauss})\left[\frac{\kappa_0 - 1 + \kappa_{\text{geo}}}{6}\right]\left(\frac{[^3\text{He}]}{1 \text{ amg}}\right)\left[\frac{P_{\text{He}}}{100\%}\right] && (33)\end{aligned}$$

3 Calculating the Shift Due to the NMR RF Field: The AC Zeeman Effect

To calculate the shift due to the AC Zeeman effect, we'll follow and in some cases generalize the basic arguments found in problem 2.7 of [7]. Since we are only interested in a given Zeeman transition within the EPR spectrum, we'll focus only on the states involved in the transition. This results in a two state system ($|m\rangle$ & $|m-1\rangle$) with a Hamiltonian written as:

$$\mathcal{H}_0 = \hbar\omega_0 F_z \tag{34}$$

where F_z is the z-component of the total atomic angular momentum, $\hbar$ is the Planck constant divided by 2π, and ω_0 is the EPR frequency for the transition for a magnetic field B_0. If another much smaller magnetic field $B_1 \ll B_0$ is turned on, then we can write the additional Zeeman interaction as:

$$\mathcal{H}_1 = -\mu \cdot \vec{B}_1 = -g\mu_B \vec{F} \cdot \vec{B}_1 \tag{35}$$

where g is the effective or Landé g-factor, μ_B is the Bohr magneton, and $\vec{F}$ is the total atomic angular momentum. In general, g depends on the total magnetic field in the z-direction, the hyperfine manifold F, and the magnetic substate m. Its form can be obtained by considering the case when $\vec{B}_1$ is in the z-direction (the same direction as $\vec{B}_0$). In this case, the total Hamiltonian can be written in two ways:

$$\mathcal{H} = \mathcal{H}_0 + \mathcal{H}_1 = \hbar\omega F_z = \hbar\omega_0 F_z - g\mu_B F_z B_1 \tag{36}$$

Taylor expanding $\omega = \omega(B_0 + B_1)$ about B_0 gives:

$$\omega(B_0 + B_1) = \omega(B_0) + (B_0 + B_1 - B_0)\frac{\partial\omega}{\partial B} = \omega_0 + B_1\frac{\partial\omega}{\partial B} \tag{37}$$

Putting this together gives the form of the effective g-factor:

$$\hbar\omega F_z - \hbar\omega_0 F_z = -g\mu_B F_z B_1 \quad \rightarrow \quad g = -\left(\frac{\hbar}{\mu_B}\right)\frac{\partial\omega}{\partial B} \tag{38}$$

where the derivative is evaluated at B_0.

We'll now consider the case of an oscillating RF field in the x-direction:

$$\mathcal{H} = \hbar\omega_0 F_z - g\mu_B F_x B_{\mathtt{rf}} \cos(\omega_{\mathtt{rf}} t) \tag{39}$$

where $B_{\mathtt{rf}}$ is the amplitude of the RF field in the lab frame and $\omega_{\mathtt{rf}}$ is the angular frequency of the RF field. In general, the non-zero matrix elements of F_z and $F_x = (F_+ + F_-)/2$ are:

$$\langle m|\, F_z\, |m\rangle = m \quad \langle m-1|\, F_z\, |m-1\rangle = m-1 \quad \langle m-1|\, F_x\, |m\rangle = \langle m|\, F_x\, |m-1\rangle = \frac{\sqrt{F(F+1)-m(m-1)}}{2} \tag{40}$$

Using these formulas, we can rewrite the Hamiltonian using the Pauli spin matrices:

$$\mathcal{H} = \hbar\omega_0\bar{m} + \hbar\omega_0\sigma_z/2 + \hbar\Omega_{\mathtt{rf}}\sigma_x\cos(\omega_{\mathtt{rf}}t)/2 \tag{41}$$

where $\bar{m} = m - 1/2$ is the mean m associated with the transition and $\Omega_{\mathtt{rf}}$ is given by:

$$\Omega_{\mathtt{rf}} = \frac{\partial\omega}{\partial B} B_{\mathtt{rf}} \sqrt{F(F+1)-m(m-1)} \tag{42}$$

Since $\hbar\omega_0\bar{m}$ is an overall constant energy offset, we can safely drop it from the Hamiltonian. For convenience, we'll relabel two eigenstates of $\mathcal{H}_0$ as $|a\rangle = |m\rangle$ and $|b\rangle = |m-1\rangle$. The eigenstates of the full Hamiltonian $\mathcal{H}$ are denoted as $|1\rangle$ & $|2\rangle$ and can be expanded as:

$$|1\rangle = a_1\exp(-i\omega_0 t/2)\,|a\rangle + b_1\exp(+i\omega_0 t/2)\,|b\rangle \qquad |2\rangle = a_2\exp(-i\omega_0 t/2)\,|a\rangle + b_2\exp(+i\omega_0 t/2)\,|b\rangle \tag{43}$$

where orthonormality enforces:

$$|a_1|^2 + |b_1|^2 = |a_2|^2 + |b_2|^2 = 1 \qquad a_1^* a_2 + b_1^* b_2 = 0 \tag{44}$$

Because we've chose to expand $|1\rangle$ & $|2\rangle$ in this way, they automatically satisfy the Schrodinger equations with $a_1 = b_2 = 1$ & $a_2 = b_1 = 0$ when there is no RF field $\Omega_{\mathtt{rf}} = 0$. Our goal now is to obtain a solution correct to the lowest order for the case when $0 < \Omega_{\mathtt{rf}} \ll \omega_0$.

Applying Schrodinger equation to $|1\rangle$, we get a pair of coupled equations:

$$\begin{aligned} i\hbar(\dot{a}_1 - i\omega_0 a_1/2)\exp(-i\omega_0 t/2) &= +(\hbar\omega_0 a_1/2)\exp(-i\omega_0 t/2) + (\hbar\Omega_{\mathtt{rf}} b_1/2)\exp(+i\omega_0 t/2)\cos(\omega_{\mathtt{rf}} t) & (45)\\ i\hbar(\dot{b}_1 + i\omega_0 b_1/2)\exp(+i\omega_0 t/2) &= -(\hbar\omega_0 b_1/2)\exp(+i\omega_0 t/2) + (\hbar\Omega_{\mathtt{rf}} a_1/2)\exp(-i\omega_0 t/2)\cos(\omega_{\mathtt{rf}} t) & (46)\end{aligned}$$

After rearranging a few things we get:

$$\begin{aligned} \dot{a}_1 &= -(i\Omega_{\mathtt{rf}} b_1/2)\exp(+i\omega_0 t)\cos(\omega_{\mathtt{rf}} t) & (47)\\ \dot{b}_1 &= -(i\Omega_{\mathtt{rf}} a_1/2)\exp(-i\omega_0 t)\cos(\omega_{\mathtt{rf}} t) & (48)\end{aligned}$$

Since $\Omega_{\mathtt{rf}}$ is small, it's not unreasonable to assume that $|a_1| \approx 1$. In other words, we'll make the ansatz that $a_1 = \exp(-i\omega_! t)$. Using this form of a_1 allows us to directly integrate $\dot{b}_1$ to give:

$$\begin{aligned} b_1 = \int \dot{b}_1\, dt &= -(i\Omega_{\mathtt{rf}}/2)\int \exp(-i(\omega_1+\omega_0)t)\cos(\omega_{\mathtt{rf}} t)\, dt & (49)\\ &= -(i\Omega_{\mathtt{rf}}/4)\int \left[\exp(-i(\omega_1+\omega_0-\omega_{\mathtt{rf}})t) + \exp(-i(\omega_1+\omega_0+\omega_{\mathtt{rf}})t)\right] dt & (50)\\ &= -(i\Omega_{\mathtt{rf}}/4)\left[\frac{\exp(-i(\omega_1+\omega_0-\omega_{\mathtt{rf}})t)}{-i(\omega_1+\omega_0-\omega_{\mathtt{rf}})} + \frac{\exp(-i(\omega_1+\omega_0+\omega_{\mathtt{rf}})t)}{-i(\omega_1+\omega_0+\omega_{\mathtt{rf}})}\right] & (51)\\ &= \frac{\Omega_{\mathtt{rf}}}{4}\left[\frac{\exp(-i(\omega_1+\omega_0-\omega_{\mathtt{rf}})t)}{\omega_1+\omega_0-\omega_{\mathtt{rf}}} + \frac{\exp(-i(\omega_1+\omega_0+\omega_{\mathtt{rf}})t)}{\omega_1+\omega_0+\omega_{\mathtt{rf}}}\right] & (52)\end{aligned}$$

Using this solution for b_1 and the ansatz for a_1, we can now apply the equation for $\dot{a}_1$:

$$\begin{aligned}
\dot{a}_1 &= -(i\Omega_{\mathtt{rf}} b_1/2)\exp(+i\omega_0 t)\cos(\omega_{\mathtt{rf}} t) && (53)\\
-i\omega_1 \exp(-i\omega_1 t) &= -i\frac{\Omega_{\mathtt{rf}}^2}{8}\exp(+i\omega_0 t)\cos(\omega_{\mathtt{rf}} t)\left[\frac{\exp(-i(\omega_1+\omega_0-\omega_{\mathtt{rf}})t)}{\omega_1+\omega_0-\omega_{\mathtt{rf}}}+\frac{\exp(-i(\omega_1+\omega_0+\omega_{\mathtt{rf}})t)}{\omega_1+\omega_0+\omega_{\mathtt{rf}}}\right] && (54)\\
\omega_1 &= \frac{\Omega_{\mathtt{rf}}^2}{8}\cos(\omega_{\mathtt{rf}} t)\left[\frac{\exp(+i\omega_{\mathtt{rf}} t)}{\omega_1+\omega_0-\omega_{\mathtt{rf}}}+\frac{\exp(-i\omega_{\mathtt{rf}} t)}{\omega_1+\omega_0+\omega_{\mathtt{rf}}}\right] && (55)\\
&= \frac{\Omega_{\mathtt{rf}}^2}{16}\left[\exp(+i\omega_{\mathtt{rf}} t)+\exp(-i\omega_{\mathtt{rf}} t)\right]\left[\frac{\exp(+i\omega_{\mathtt{rf}} t)}{\omega_1+\omega_0-\omega_{\mathtt{rf}}}+\frac{\exp(-i\omega_{\mathtt{rf}} t)}{\omega_1+\omega_0+\omega_{\mathtt{rf}}}\right] && (56)\\
&= \frac{\Omega_{\mathtt{rf}}^2}{16}\left[\frac{1+\exp(+2i\omega_{\mathtt{rf}} t)}{\omega_1+\omega_0-\omega_{\mathtt{rf}}}+\frac{1+\exp(-2i\omega_{\mathtt{rf}} t)}{\omega_1+\omega_0+\omega_{\mathtt{rf}}}\right] && (57)\\
& && (58)
\end{aligned}$$

Our first approximation will be to drop the rapidly oscillating terms to get:

$$\omega_1 = \frac{\Omega_{\mathtt{rf}}^2}{8}\left[\frac{\omega_1+\omega_0}{(\omega_1+\omega_0)^2-\omega_{\mathtt{rf}}^2}\right] \quad (59)$$

Our second approximation is that $\omega_1 \ll \omega_0$, which allows us to solve for ω_1:

$$\begin{aligned}
\omega_1 &= \frac{\Omega_{\mathtt{rf}}^2}{8}\left[\frac{\omega_0}{\omega_0^2-\omega_{\mathtt{rf}}^2}\right]\left[1+\frac{\omega_1}{\omega_0}\right]\left[1+\frac{2\omega_1\omega_0+\omega_1^2}{\omega_0^2-\omega_{\mathtt{rf}}^2}\right]^{-1} && (60)\\
&\approx \frac{\Omega_{\mathtt{rf}}^2}{8}\left[\frac{\omega_0}{\omega_0^2-\omega_{\mathtt{rf}}^2}\right]\left[1-\frac{\omega_1}{\omega_0}\left(\frac{\omega_0^2+\omega_{\mathtt{rf}}^2}{\omega_0^2-\omega_{\mathtt{rf}}^2}\right)\right] && (61)\\
&= \frac{\Omega_{\mathtt{rf}}^2}{8}\left[\frac{\omega_0}{\omega_0^2-\omega_{\mathtt{rf}}^2}\right]\left[1+\frac{\Omega_{\mathtt{rf}}^2(\omega_0^2+\omega_{\mathtt{rf}}^2)}{8(\omega_0^2-\omega_{\mathtt{rf}}^2)^2}\right]^{-1} && (62)
\end{aligned}$$

For self-consistency, this approximation necessarily implies that $\Omega_{\mathtt{rf}} \ll \omega_0$ which is roughly equivalent to our earlier assertion that $B_{\mathtt{rf}} \ll B_0$. Our third and final approximation is that the frequency of the RF field is far from resonance, $\omega_{\mathtt{rf}} \ll \omega_0$, which finally gives:

$$\omega_1 = \frac{\Omega_{\mathtt{rf}}^2}{8}\left[\frac{\omega_0}{\omega_0^2-\omega_{\mathtt{rf}}^2}\right]\left[1+\frac{\Omega_{\mathtt{rf}}^2(\omega_0^2+\omega_{\mathtt{rf}}^2)}{8(\omega_0^2-\omega_{\mathtt{rf}}^2)^2}\right]^{-1} \approx \frac{\Omega_{\mathtt{rf}}^2}{8\omega_0} \quad (63)$$

We can follow this same calculation for $|2\rangle$ where a_2 plays the same role as b_1, b_2 plays the same role as a_1, and we must flip the sign of ω_0:

$$\begin{aligned}
a_2 &= \frac{\Omega_{\mathtt{rf}}}{4}\left[\frac{\exp(-i(\omega_2-\omega_0-\omega_{\mathtt{rf}})t)}{\omega_2-\omega_0-\omega_{\mathtt{rf}}}+\frac{\exp(-i(\omega_2-\omega_0+\omega_{\mathtt{rf}})t)}{\omega_2-\omega_0+\omega_{\mathtt{rf}}}\right] && (64)\\
b_2 &= \exp(-i\omega_2 t) && (65)\\
\omega_2 &\approx -\frac{\Omega_{\mathtt{rf}}^2}{8\omega_0} && (66)
\end{aligned}$$

Putting this altogether gives:

$$\begin{aligned}
|1\rangle &= \exp(-i(\omega_0/2+\omega_1)t)\,|a\rangle + b_1\exp(+i\omega_0 t/2)\,|b\rangle && (67)\\
|2\rangle &= a_2\exp(-i\omega_0 t/2)\,|a\rangle + \exp(+i(\omega_0/2-\omega_2)t)\,|b\rangle && (68)\\
b_1 &= +\frac{\Omega_{\mathtt{rf}}}{4\omega_0}\exp(-i(\omega_1+\omega_0)t)\cos(\omega_{\mathtt{rf}} t) && (69)\\
a_2 &= -\frac{\Omega_{\mathtt{rf}}}{4\omega_0}\exp(-i(\omega_2-\omega_0)t)\cos(\omega_{\mathtt{rf}} t) && (70)\\
\omega_1 = -\omega_2 &= \frac{\Omega_{\mathtt{rf}}^2}{8\omega_0} && (71)
\end{aligned}$$

B_0 Gauss	isotope	I	m $\pm[I]/2$	ν_0 MHz	$\partial\nu/\partial B$ kHz/G	$(\Delta\nu)_{\mathtt{rf}}$ kHz/G^2	$(\Delta\nu)_{\mathrm{He}}$ kHz/amg
13	^{85}Rb	5/2	+3	6.01	458	52.4	−7.08
			−3	6.13	476	55.4	+7.36
	^{39}K	3/2	+2	8.59	622	45.0	−9.01
			−2	9.67	788	64.2	+11.4
23	^{85}Rb	5/2	+3	10.55	451	28.9	−6.97
			−3	10.93	484	32.1	+7.48
	^{39}K	3/2	+2	14.54	569	22.3	−8.24
			−2	17.91	863	41.6	+12.5

Table 2: EPR Frequency Shifts for the End Transitions Due to the NMR RF Field & Polarized ^{3}He. We've assumed that $B_{\mathtt{rf}} \ll B_0$ and $\nu_{\mathtt{rf}} \ll \nu_0$. The $-(+)$ sign for m refers to the "well" ("hat") state. For the shift due to the polarized ^{3}He, we've assumed a spherical sample at a temperature of 200 °C and 100% polarization. The sign of the polarization is taken to be the same as the sign of the alkali m state.

To lowest order, the energy levels are:

$$\langle 1|\,\mathcal{H}\,|1\rangle = \langle 1|\,i\hbar\frac{\partial\,|1\rangle}{\partial t} \approx +\hbar(\omega_0/2+\omega_1) \tag{72}$$

$$\langle 2|\,\mathcal{H}\,|2\rangle = \langle 2|\,i\hbar\frac{\partial\,|2\rangle}{\partial t} \approx -\hbar(\omega_0/2-\omega_2) \tag{73}$$

and finally the frequency is:

$$\omega = \frac{\langle 1|\,\mathcal{H}\,|1\rangle - \langle 2|\,\mathcal{H}\,|2\rangle}{\hbar} = \omega_0+\omega_1-\omega_2 = \omega_0+\frac{\Omega_{\mathtt{rf}}^2}{4\omega_0} = \omega_0\left[1+\left(\frac{\partial\omega}{\partial B}\frac{B_{\mathtt{rf}}}{2\omega_0}\right)^2(F(F+1)-m(m-1))\right] \tag{74}$$

The AC Zeeman frequency shift due to an RF field for the transition $|F,m\rangle \leftrightarrow |F,m-1\rangle$ when $B_{\mathtt{rf}} \ll B_0$ and $\nu_{\mathtt{rf}} \ll \nu_0$ is, to lowest order, given by:

$$(\Delta\nu)_{\mathtt{rf}} = \frac{F(F+1)-m(m-1)}{4\nu_0}\left[\frac{\partial\nu}{\partial B}B_{\mathtt{rf}}\right]^2 \tag{75}$$

where $B_{\mathtt{rf}}$ is the magnitude of the RF field in the lab frame, ν_0 is the frequency of the transition when $B_{\mathtt{rf}} = 0$, and the derivative for $F = I \pm 1/2$ is given by (up to fifth order in field) Eqn. (9). For the special case of end transitions, $F = I+1/2$ and $m = I+1/2$ for $I+1/2 \leftrightarrow I-1/2$ & $m = -I+1/2$ for $-I+1/2 \leftrightarrow -I-1/2$ and the frequency shift is:

$$(\Delta\nu)_{\mathtt{rf}} = \frac{[I]}{4\nu_0}\left[\frac{\partial\nu}{\partial B}B_{\mathtt{rf}}\right]^2 \tag{76}$$

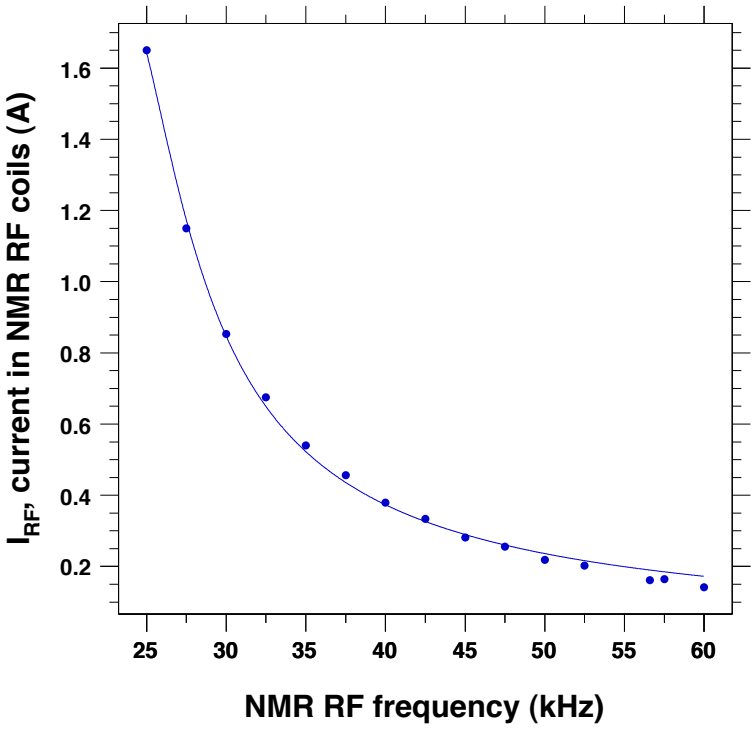

Figure 3: Current in NMR RF coils for a set amplitude of $V_{\text{set}} = 300$ mV. The NMR RF coils resonate at about 20 kHz.

4 An Experimental Study of the NMR RF Shift Effect

To study the NMR RF Shift effect, we took data for:

1. fields of 13 Gauss and 23 Gauss
2. NMR RF frequencies of 25.0 kHz, 30.0 kHz, 35.0 kHz, and 56.6 kHz
3. NMR RF set amplitude from 25 mV up to 600 mV or whatever value the NMR RF amplifier would overload
4. ^{39}K in the "well" state

At typical sequence is depicted in Fig. (4). For each data set, we would measure the EPR frequency, the current in the Helmholtz coils, and the current in the NMR RF coils. For all of the measurements, the current in the Helmholtz coils was very stable and the ^{3}He polarization had reached equilibrium. Therefore any change in the EPR frequency was mostly due to the NMR RF field.

After collecting this data, we plot the shift vs. NMR RF set amplitude, see Fig. (5). The expected quadratic behavior is readily seen. We don't expect the NMR RF frequency to play a direct role in the shift. Therefore we measured the current in the NMR RF coils vs. NMR RF frequency for a fixed set amplitude V_{set}, see Fig. (3). To make all the data comparable, we convert the shift into the amplitude of the RF field causing it using Eqn. (76). Since the same set amplitude doesn't correspond to the same current in the NMR RF coils for different NMR RF frequencies, we plot the data vs. the current in the RF coils instead. When we do this, if our calculation is correct, then all the data should lie on a line. To better than 5%, this is true and we get a slope of 182 mG/A.

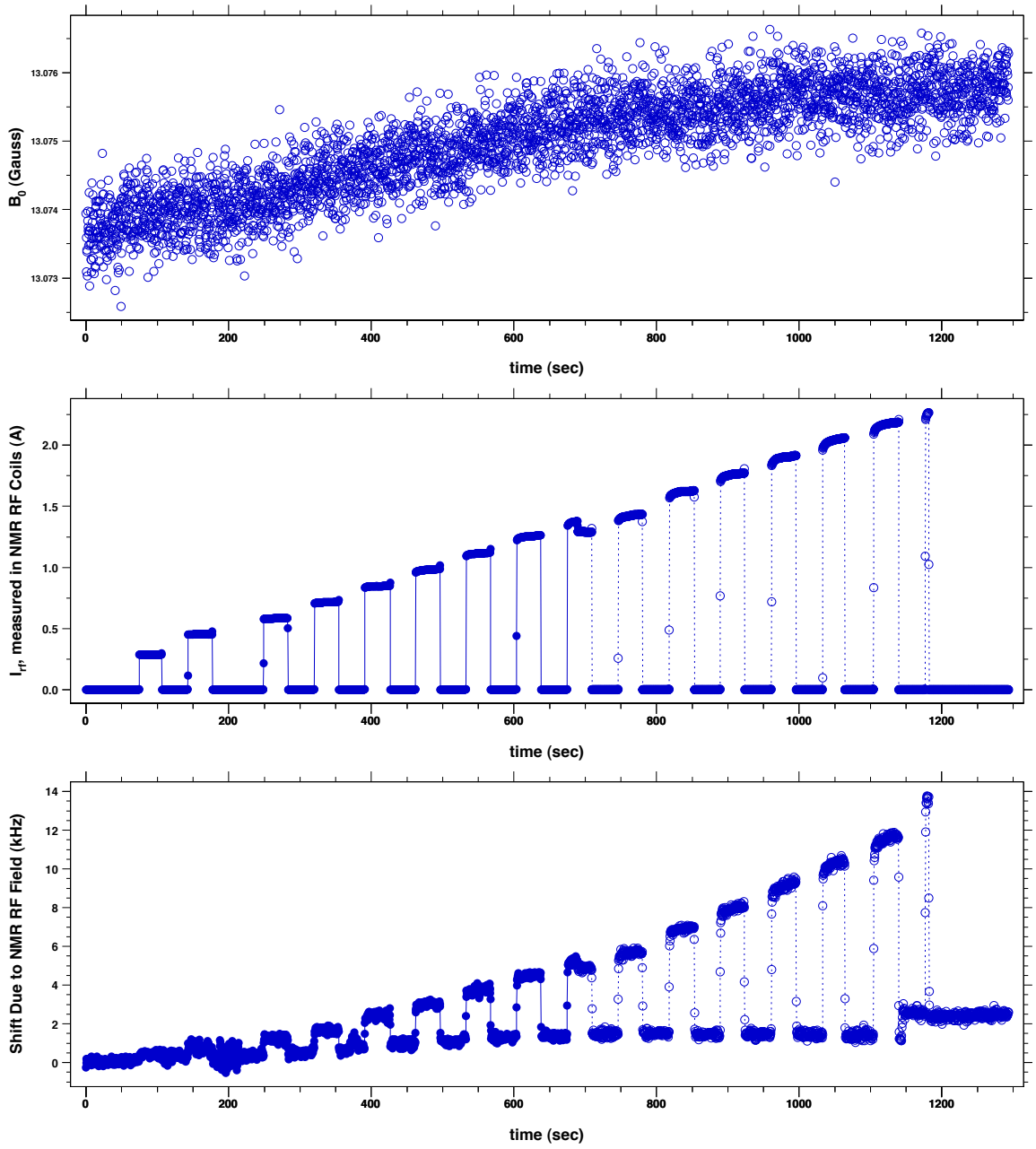

Figure 4: Shift in the EPR Frequency for an NMR RF Field at 25 kHz. The top plot shows the magnitude of the holding field as measured from the current in the Helmholtz coils. Over the course of the measurement, it was stable to a few milligauss. The middle plot shows the current in NMR RF coils. During the measurement, the RF field was turned off and on at linearly increasing amplitudes. The bottom plot shows the locked EPR frequency as the NMR RF field is varied. The measurement was done at the end of a spin-up, so we assume that the ^{3}He polarization was at equilibrium. The field due to the polarized ^{3}He is about 40 milligauss, which corresponds to a frequency shift of about 30 kHz. The magnitude of the NMR RF field is increased linearly, whereas the shift is increasing in a quadratic manner. At around $t = 700$ sec, there was a glitch in the RF amplitude. In addition, the NMR RF amplifier overloaded at around $t = 1175$ sec. Both of these features can be seen in both the bottom two plots.

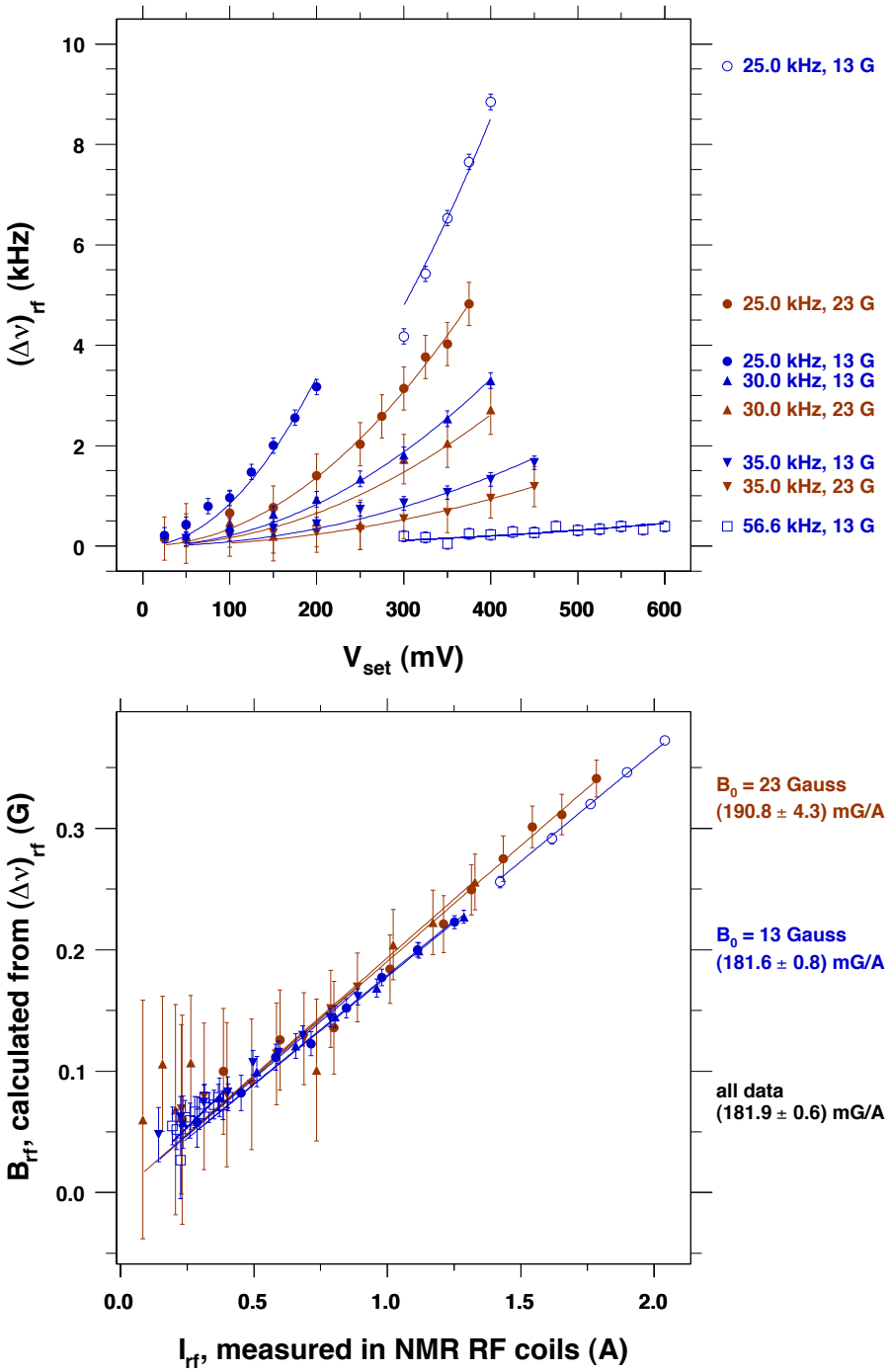

Figure 5: Measurement of $(\Delta\nu)_{\mathtt{rf}}$ under different conditions. We measured the NMR RF shift at two different fields, four different NMR RF frequencies, and several NMR RF field amplitudes. The top plot shows the shift plotted against set amplitude. Except for the 25.0 kHz, 13 Gauss data set, there was a linear relationship between the current in the NMR RF coils and the set amplitude. For the 25.0 kHz, 13 gauss data set, a glitch occurred during the measurement, see Fig. (4). For the bottom plot, we've inserted the measured shift into Eqn. (76) and solved for the amplitude of the NMR RF field in the lab frame. Once this value for $B_{\mathtt{rf}}$ is plotted against the measured current $I_{\mathtt{rf}}$ in the NMR RF coils, the data cluster along a line.

References

[1] S. R. Schaefer, G. D. Cates, Ting-Ray Chien, D. Gonatas, W. Happer, and T. G. Walker. Frequency shifts of the magnetic-resonance spectrum of mixtures of nuclear spin-polarized noble gases and vapors of spin-polarized alkali-metal atoms. *Physical Review A*, 39(11):5613–5623, Jun 1989.

[2] N. R. Newbury, A. S. Barton, P. Bogorad, G. D. Cates, M. Gatzke, H. Mabuchi, and B. Saam. Polarization-dependent frequency shifts from Rb-^{3}He collisions. *Physical Review A*, 48(1):558–568, Jul 1993.

[3] A. S. Barton, N. R. Newbury, G. D. Cates, B. Driehuys, H. Middleton, and B. Saam. Self-calibrating measurement of polarization-dependent frequency shifts from Rb-^{3}He collisions. *Physical Review A*, 49(4):2766–2770, Apr 1994.

[4] M. V. Romalis and G. D. Cates. Accurate ^{3}He polarimetry using the Rb Zeeman frequency shift due to the Rb-^{3}He spin-exchange collisions. *Physical Review A*, 58(4):3004–3011, Oct 1998.

[5] Earl Babcock, Ian A. Nelson, Steve Kadlecek, and Thad G. Walker. ^{3}He polarization-dependent EPR frequency shifts of alkali-metal-^{3}He pairs. *Physical Review A*, 71(1):013414, Jan 2005.

[6] John David Jackson. *Classical Electrodynamics*. John Wiley & Sons, New York, 3rd edition, 1999.

[7] Dmitry Budker, Derek K. Kimball, and David P. DeMille. *Atomic Physics: An Exploration Through Problems and Solutions*. Oxford University Press, Oxford, Great Britain, 1st edition, 2004.